III International Conference on Particle-based Methods – Fundamentals and Applications
PARTICLES 2013
M. Bischoff, E. Oñate, D.R.J. Owen, E. Ramm & P. Wriggers (Eds)

ON ELASTICITY OF SPRING NETWORK MODELS USED IN BLOOD FLOW SIMULATIONS IN ESPRESSO*

I. CIMRÁK[1], I. JANČIGOVÁ[2], K. BACHRATÁ[2], AND H.BACHRATÝ[1]

[1] Department of Software Technologies, University of Žilina
Univerzitná 8215/1, 01026 Žilina, Slovakia
ivan.cimrak/hynek.bachraty@fri.uniza.sk, http://www.kst.fri.uniza.sk/~icimrak

[2] Department of InfoCom Networks, University of Žilina
Univerzitná 8215/1, 01026 Žilina, Slovakia
iveta.jancigova/katarina.bachrata@fri.uniza.sk, http://www.kis.fri.uniza.sk

Key words: LBM, Immersed bondary method, fluid flows, immersed objects, ESPResSo

Abstract. For the proper simulation of processes inside microfluidic devices, proper model for blood flow must be used. We use the lattice-Boltzmann method for the blood plasma flow and the immersed boundary method for the description of red blood cells and other components of blood. One of the four key mechanisms governing the elastic behaviour of a red blood cell is the in-plane shear modulus of elasticity.

The membrane of red blood cell is modeled with a triangular network of springs with stretching coefficient k. Physical properties of the membrane is given by the in-plane shear modulus of elasticity μ. We study the dependence of the stretching coefficients of the springs on the in-plane shear modulus. First we derive analytical results for regular two dimensional networks. For networks, or meshes, covering the surface of three dimensional objects we first define the mesh density. Then we state the hypothesis deriving the relation between μ and k and finally we verify the hypothesis by numerous simulations.

1 INTRODUCTION

The simulation of elastic objects immersed in a fluid is a key approach in numerous applications ranging from small-scale simulations, e.g. blood flow modelling, or patogene tracking, to large scale simulations including for example flood simulations. Our focus is on blood flow modelling where blood is considered as a suspension of liquid blood plasma and elastic objects such as red and white blood cells, platelets, circulating tumour cells.

*This work was supported by the Slovak Research and Development Agency under the contract No. APVV-0441-11, by the Marie-Curie grant No. PCIG10-GA-2011-303580, and by the Action Austria-Slovakia grant No. 2012-03-15-0003.

1.1 Model

Our model consists of two pricipal parts. The fluid is modeled by the lattice-Boltzmann (LB) method and the immersed objects are approximated by the immersed boundary (IB) method.

Fluid. In the LB method, the fluid is represented by fictive particles that can move along the edges of fixed lattice [1]. Velocity, density and pressure in the fluid can be expressed using suitable averages of fictive particles in the lattice nodes.

This approach is recently very popular and it has some advantages compared to conventional Navier-Stokes equations. Low Reynolds number in simulations of microfluidic devices guarantees that numerical instabilities can be solved e.g. by decreasing the time discretization.

Immersed objects. For the description of immersed objects we choose the immersed boundary (IB) method [6]. This method represents an elastic object by its boundary which is triangulated with a mesh. Each node in the mesh is called the IB node and moves freely in the 3D space, its movement is not restricted to any lattice. However, there are bonds defined between the neighbouring nodes in the mesh. These bonds create forces that are applied to these nodes and these forces are responsible for e.g. keeping the shape of the object, for bending and stretching of the object, and for other elastic forces.

Each time step, all the forces acting on one IB point are summed up. The resulting force causes that IB point moves and this movement is governed by Newton equations of motion. This way the whole object moves and deforms.

Fluid-objects interaction. The fluid and the immersed objects interact with each other. This interaction must be implemented to approximate the real flow fluid with objects. Currently, we use the drag-force approach [2].

1.2 Microfluidic devices

The overall focus of our research, the partial results of which we will make known to you in the following, is development in simulation of microfluidic devices. Their purpose is capturing circulating tumor cells (CTCs) from blood [7]. These are modern devices that make possible a comfortable and non-invasive method for the diagnosis of various cancers and the monitoring of their treatment. The main requirement for their real-life implementation, and also the challenge of research in this area, is the need for an effective method of capturing CTCs. These are present in blood plasma in a ratio of 1:1 000 000 to red blood cells, which form the chief component of its solid content, and an analyzed blood sample typically only contains a few dozen CTCs. Therefore, the high effectiveness of CTC capture is crucial. In this article we address the implementation of a simulation method in software package ESPResSo [2].

For the accurate simulation we need to include many aspects in the model. The basic attributes of the flow are its speed and shear stress, and for the particles contained within also the duration of contact with the surface of the device and method of flowing around

microposts. These attributes are key to efficiency in capturing CTCs. Therefore it is a matter of course to attempt to optimize the shape and topology of the devices. Here we run into practical problems. Even though prototype microfluidic devices exist and function, their manufacture and especially optimization through experimental means is too expensive and slow. An effective substitute in this situation are the methods of computer simulation and the optimization methods based on such. However, the complexity of the problems does not permit simply using existing and known software tools. To the contrary, it is the impetus for titillating research at the boundaries of computer science, mathematics, physics, and biology, in which we are attempting to participate.

The complex problem of simulating the attributes and abilities of microfluidic chambers can be divided into several interconnected areas.

a) Modelling the flow of a fluid through chambers of various shapes

b) Elastic models of particles within blood plasma

c) The interaction of fluid flow and the particles contained therein

d) Modelling the adhesion of CTC cells on the surface of the devices

e) Mastering and realization of computing-intensive simulations

f) Correctly estimating the necessary degree of accuracy of utilized models

The first two are present also in this work and have been detailed in Section 1.1. The remaining areas will be discuseed in forthcoming articles.

1.3 Elastic constraints

For proper representation of an immersed object we need to define the forces in each IB node. These forces keep the shape of the object, are responsible for elastic behaviour, resolve the collisions between different objects. Our main concern are the elastic properties of the object. Since the main focus of our current research is to model the blood flow in microfluidic devices, we study the elastic properties of red blood cells.

Red blood cells (RBCs) are biconcave disks with a rest shape. This shape is mantained by two structural membrane components: the plasma membrane and the cytoskeleton. The plasma membrane is responsible for a resistance to surface area dilatation. The cytoskeleton, on the other hand, is a triangular protein network, that acts like a triangular network of springs, providing viscoelastic resistance to bending and stretching of the membrane.

There are four mechanisms that affect the energy and therefore the shape of the membrane [4]. Preservation of the inner volume, preservation of the surface area, stretching of the membrane and bending of the membrane. Each of these mechanisms is represented by a specific modulus. The physical values are $0.033\mu\mathrm{N\,s\,cm^{-1}}$ for the volume compresibility

modulus, 5×10^5pNμm^{-1} for the area compresibility modulus, 5pNμm^{-1} for the stretching modulus and 10^{-1}pNμm^{-1} for the bending modulus.

In the model, each of these mechanisms is implemented through a particular force. We thus distinguish between volume and area conservation forces, the stretching force and the bending force. The actual expressions for the forces are taken from [4]. For detailed description of these forces we refer to our earlier article [3].

In this work we solely focus on the stretching force F. This force acts between two IB nodes joined with an edge in the triangulation mesh. Given the coordinates of two IB points one can compute the current distance L_c between these points. The force is defined as an elastic spring with predefined relaxed length L. If $L_c = L$ then no force acts on the IB points. When $L_c < L$ then F is repulsive and if $L_c > L$ then F is attractive. Denoting $\Delta L = L_c - L$ the relation reads as

$$F = k\frac{\Delta L}{L}. \tag{1}$$

2 STRETCHING CALIBRATION

We are concerned about the elastic shear modulus μ of a material. In general, this modulus μ is defined as a ratio between shear stress σ and strain ϵ. In three dimensions consider the elastic prolongation of a rod in longitudinal direction. Here the relation for stress reads $\sigma = F/A$ with F being the force acting on the end of the rod and A being the cross-sectional area of the rod. The strain is defined as a relative prolongation $\epsilon = \Delta L/L$ with L being the relaxed length of the red and ΔL its prolongation. The elastic shear modulus μ can be expressed as

$$\mu = \frac{F/A}{\Delta L/L} = \frac{F\cdot L}{A\cdot\Delta L} \tag{2}$$

In case of a rectangular elastic sheet with constant thickness, the problem becomes two dimensional. The cross-sectional area A is replaced by the cross-sectional length d_A. The relation for the in-plane shear modulus becomes

$$\mu = \frac{F\cdot L}{d_A\cdot\Delta L} \tag{3}$$

We model membrane by a triangular mesh of springs therefore we expect that the elastic properties of the mesh should copy those of a membrane. In Section 1.3 we state the equation (1) of the force between two points in a stretched net of springs. Consequently, the stretching coefficient is equal to

$$k = \frac{F\cdot L}{\Delta L}. \tag{4}$$

Note how the expressions for elastic modulus changed. In three dimensions in (2), we have the cross-sectional area A. In two dimensions we have the cross-sectional length of

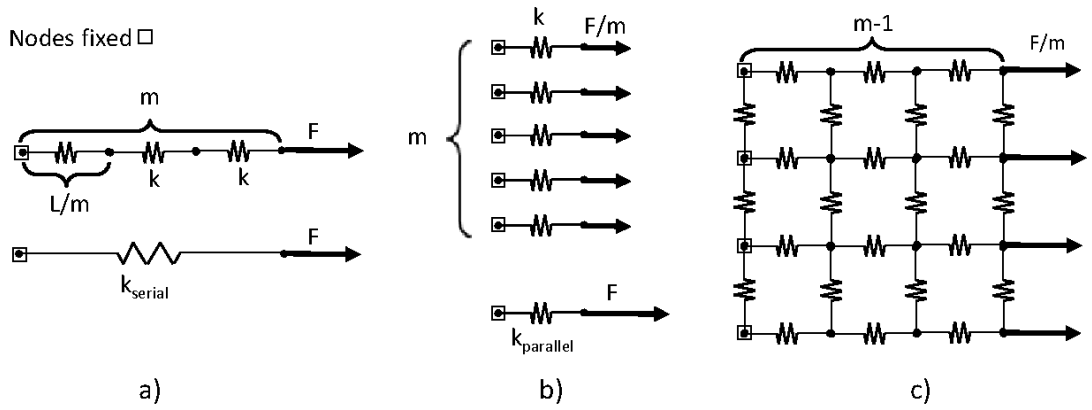

Figure 1: Replacement of m-springs system by a single spring in a) serial and b) parallel cases. c) Square lattice of $2m(m-1)$ springs.

the sheet. The spring is one dimensional object and therefore this normalization term does not have sense. It is replaced by the density of the mesh.

In the following we study this dependence and we suggest a methodology how to determine correct stretching coefficient for the springs such that physical value of the in-plane shear modulus is reconstructed.

In Section 2.1 we focus on regular meshes. We study the dependence of the stretching coefficient k on the density of regular quadrilateral and triangular meshes. In Section 2.2 we formulate the hypothesis for more general triangular meshes of the sphere. Afterwards in Section 2.3 we design an experiment that will confirm our hypothesis.

2.1 Regular meshes

The aim of this section is to derive the relation between in-plane shear modulus μ given by (3) and the stretching coefficients k defined by (4). Notice that k and μ have different units, this is caused by the fact that k is the stretching coefficient for a 1-dimensional spring and μ represents the stretching of a 2-dimensional sheet. Therefore we expect that the number of springs will play a role in the $k-\mu$ relation.

Quadrilateral mesh

If we consider a square sheet stretched in horizontal direction with in-plane shear modulus (3) and $d_A = L$, the prolongation is

$$\Delta L = \frac{F}{\mu}. \tag{5}$$

In the small deformation regime we assume that the sheet will not deform in transverse direction.

In order to compare this with a spring lattice (or mesh), first we look at the serial and parallel spring system in Figure 1 a) and b), with stretching force

$$F = k\frac{\Delta L}{L}$$

For the serial setup of m identical springs depicted in Figure 1 a), with length $L_i = \frac{L}{m}$ and stretching coefficient k, we have total $\Delta L = \sum_{i=1}^{m} \Delta L_i = \sum_{i=1}^{m} \frac{F(L/m)}{k}$. If we replace this system with one spring of length L and stretching coefficient k_{serial} and the same prolongation $\Delta L = \frac{FL}{k_{serial}}$, we have $k_{serial} = k$ regardless of m.

If we consider m identical parallel springs as depicted in Figure 1 b), the overall force F is distributed among m springs. Therefore, the force applied to one spring will be F/m. The prolongation of such spring will be according to (1) $\Delta L = \frac{L.F/m}{k}$. If we want to replace this parallel system of m springs with a single spring with stretching coefficient $k_{parallel}$ we need to equate the prolongations of both

$$\Delta L = \frac{L.F/m}{k} = \frac{L.F}{k_{parallel}}, \qquad \text{which gives} \qquad k_{parallel} = mk.$$

Now consider the square lattice of springs with $e = 2m(m-1) \sim 2m^2$ springs, see Figure 1 c). Note, that if the forces are applied in the horizontal direction, the spring lattice will not shrink in the vertical direction. Thus, for a square with e springs, each with stretching coefficient k, the prolongation of the whole system is

$$\Delta L = \frac{L.F/m}{k}. \tag{6}$$

Equating (5) and (6), we see that the stretching coefficient of the spring and physical in-plane shear modulus are related through the "spring density"

$$\mu = \frac{m}{L}k \sim \frac{\sqrt{e/2}}{L}k. \tag{7}$$

Triangular mesh

Now consider a regular triangular lattice of length L with individual spring length $L_i = L/m$. In this case, the horizontal stretching of the lattice will cause transverse shrinking. However, we would like to study only horizontal prolongations and therefore we assume that the IB nodes are not allowed to move in vertical direction. This simplification can only be done in the small deformations regime.

In the following, we will treat all the springs as horizontal springs. The originally horizontal springs are treated the same way as the horizontal springs in the square lattice. For the tilted springs, we consider the following simplification: we replace them with new rows of horizontal springs with different length and different stretching coefficient k_{repl}, see Figure 2 a) and b).

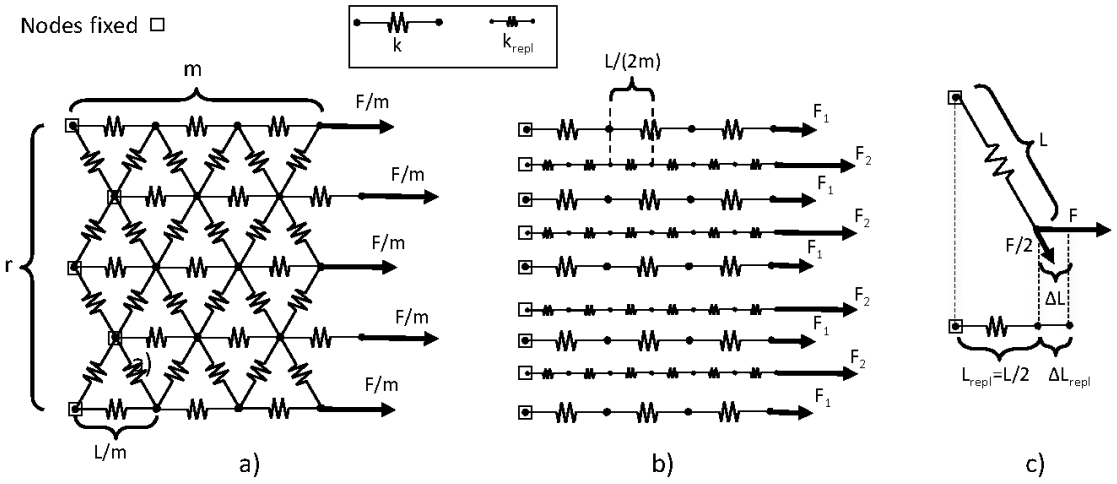

Figure 2: a) and b): Simplification of triangular spring system. c) Tilted springs are replaced with horizontal springs with length L_{repl} and stretching coefficient k_{repl}.

To determine the length of the replacement springs, we project the tilted spring onto the horizontal line and get $L_{repl} = L_i \cos\frac{\pi}{3} = \frac{L_i}{2}$. To determine their stretching coefficient, we go back to the stretching force formula (1). Since the force is applied only in horizontal direction, we compute its projection on the tilted spring line $F_{tilted} = \frac{F}{2}$, see Figure 2 c). From that we get $\Delta L_{tilted} = \frac{(F/2)L_i}{k}$ and after projection back to the horizontal direction, the prolongation of the new spring is $\Delta L_{repl} = \frac{FL_i}{4k}$. Applying relation (1) for the new spring

$$F = \frac{k_{repl}\frac{FL_i}{4k}}{\frac{L_i}{2}} \tag{8}$$

allows us to compute $k_{repl} = 2k$.
If a force F results in prolongation of ΔL in a serial system of m springs with stretching coefficient k and length L, then we need a force $2F$ to get the same prolongation ΔL in a serial system of $2m$ springs with stretching coefficient $k_{repl} = 2k$ and length $\frac{L_i}{2}$. Thus for system with a large number of rows in Figure (2) a) and b), we divide the total force F as $F_1 = \frac{F}{3m}$ and $F_2 = \frac{2F}{3m}$. The corresponding prolongation is $\Delta L = \frac{F/(3m)L}{k}$. Equating it with (5) gives us

$$\mu = \frac{3m}{L}k \sim \frac{\sqrt{e/3}}{L}k. \tag{9}$$

2.2 More general shapes

Assume that we have a triangulation of a sphere. Denote by n, e, f the number of nodes, edges and faces, respectively. Since all the faces in the mesh are triangles, we have that $2e = 3f$. Assume that this triangulation is in some sense regular and that

the triangles tend to be equilateral. Triangulations we consider are dense enough to be locally considered as a plane triangulation. Therefore in most cases each node of the triangulation has 6 edges adjacent. This leads us to $6n = 2e$. Thus the relations between the number of nodes, edges and triangles are $e = 3n$ and $f = 2/3e = 2n$. Here we see that all three quantities characterizing mesh are linearly connected.

Second important characteristic of mesh is its density. Since the meshes are subtle enough with respect to the area of triangulated surface, we can neglect some numerical irregularities caused by their borders. Then it is natural to define the density of the mesh as

$$\delta = \sqrt{\frac{e}{A}},$$

where A is the surface area. By this definition in case of large regular quadrilateral or triangular meshes discussed in Section 2.1 doubled density naturally corresponds to meshes with halved sizes of used squares or triangles, respectively. Thus the mesh density δ corresponds with its linear density in x and y directions. More precisely, there is square root dependence of density δ on the number of edges e, so for example quadrupled number of edges causes doubled mesh density.

Stiffness of the sphere. Consider a sphere shell made of an elastic material. The physical properties of the material, together with the fact that the thickness of the sphere does not change, guarantee that the elastic behaviour of the shell can be characterized by its in-plane shear modulus μ. This spherical shell will be modeled by a sphere covered with a triangular mesh with n nodes, e edges and f triangles. It is reasonable to assume that each edge in the triangulation has the same stretching coefficient given by k. The question is, whether the elastic behaviour of the simulated sphere is the same as that of the real shell.

Our next objective is to find out how μ and k are related.

It is natural to expect that when we change the mesh density with preserved k than the elastic behaviour of simulated physical object will change. The overall elastic behaviour is characterized by the in-plane shear modulus μ and therefore, it has to be a functional dependence of μ on the mesh.

We suggest that the increase in the number of edges will increase the overall stiffness of the sphere. This is a natural observation since with the increased number of edges the springs are denser. Moreover, in Section 2.1 we identified the dependencies (9) and (7) which confirm this assumption.

The in-plane shear modulus given by (3) is a quantity that is related to a surface of an object. This surface is modeled by the net of springs. For us it would be interesting to know how the in-plane modulus changes when the density of mesh is for example doubled. Further we think that if the density of mesh is doubled then the overall stiffness of the sphere is doubled too. This leads us to hypothesis that μ and k depend linearly on the density of the mesh. Moreover, the relations (9) and (7) confirm the following hypothesis.

Hypothesis 1 *Physical in-plane shear modulus μ of the sphere shell depends linearly on the mesh density δ of the underlying triangulation and on the stretching coefficient k of the springs. More specifically, there exists dimensionless parameter C such that*

$$\mu = C.\delta.k. \tag{10}$$

Two quantities k and μ in (10) do not have same units. Their definitions (3) and (4) determine that $[\mu] = \mathrm{m}^{-1}[k]$. Since $[\delta] = \mathrm{m}^{-1}$ the relation (10) is consistent with previous developments assuming that C is dimensionless.

Remark 1 *It is not our aim to derive rigorous expressions. The relation (10) is not exact. The true dependence of μ on the mesh is much more complicated and even small changes in the mesh will influence this dependence. However we aim to derive a guidelines how to pick up the right approximation of the in-plane shear modulus when we attempt to simulate fluidic processes using our implementation in ESPResSo. It is possible to consider different stretching coefficient for each spring in the triangular mesh. The analysis on this topic can be found in [5, 10].*

2.3 Verification of the hypothesis

We consider the following experiment, see Figure 3. A spherical shell with constant thickness is stretched with two opposite forces applied at its north and south pole. We only consider the linear elasticity limit in the small deformation regime. According to [8, 9], the deformation of the diameter along the equator will be

$$D = D_0 - \frac{F}{2\pi\mu}, \tag{11}$$

where D_0 is the diameter of the sphere in the relaxed state, D is the diameter of stretched sphere in equilibrium, F is the applied force and μ is the in-plane shear modulus.

For a given spherical shell with diameter D_0 we take the reference mesh. For this mesh we can compute its mesh density δ. In real experiments we would like to model a shell

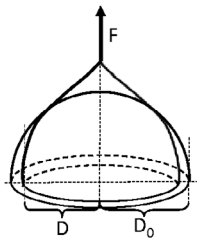

Figure 3: Set up for the experiment. The upper half sphere with initial diameter D_0 is stretched by its north pole with force F. In the equilibrium, diameter shrinks to D according to (11).

with given in-plane shear modulus so we pick some value for μ. From (11) we know how the diameter of the shell shrinks when stretched by force F. So we pick some value of F, we simulate the stretching and we measure the diameter. Our last remaining parameter k wil be identified such that simulated diameter corresponds to precomputed diameter from (11). Once we have correct k such that simulated and precomputed diameters of shrunked sphere are the same, we are able to determine $C = \mu/(\delta.k)$.

2.4 Consistency

If Hypothesis 1 is correct, C should be independ of other parameters in the model. Therefore we must test whether C changes when we take different values for the parameters.

First attempt to test our software implementation is to make sure that C does not change for different values of k or for changing of stretching force F. We ran series of simulations for a fixed mesh with 601 nodes. For this mesh we fixed the force to a specific value and we ran simulations for different values of k. Figure 4 left illustrates the identification of C from these simulations.

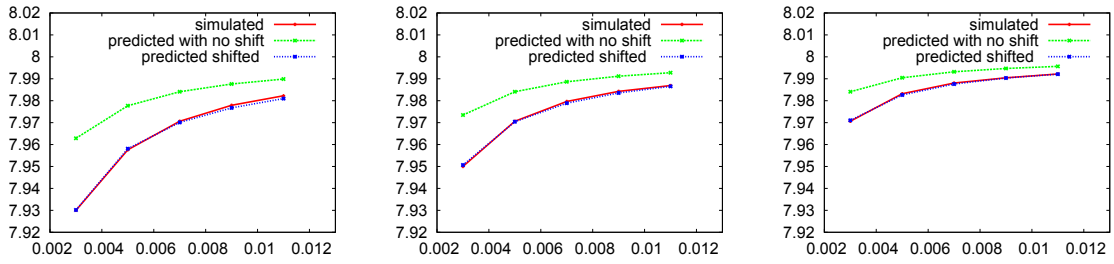

Figure 4: Mesh with $n = 601$, k ranging from 0.003 to 0.011 and stretching force with $F = 0.0007$ on the left, $F = 0.0005$ in the middle and $F = 0.0003$ on the right. The diameter of the simulated sphere is represented by the red full line. We computed diameter with no shift predicted from (11) with $\mu = k$. We obtained the green dashed line. Obviously the red full line and the green dashed line do not coincide. We identified correct value of C for each force separately and we computed shifted diameter predicted from (11) with $\mu = C\delta k$. We obtained the blue dotted line. Now the blue dotted line and the red full line coincide.

Next we changed the stretching force several times and for each of these forces we ran the set of simulations with k changing. In Figure 4 we see the snapshots of these tests. The expected result was that the identified C will be the same for all these results. In Table 1 we see that for forces $F = 0.0007, 0.0005, 0.0003$ the identified values of $C = 0.178, 0.180, 0.184$.

The previous test of consistency we ran for numerous other meshes. Table 1 shows the values of identified C. Although the identified C changes a little bit, the changes are not dramatic. In view of Remark 1 we conclude that our model is consistent with respect to changes in k and stretching force F.

n	F	C	n	F	C
304	0.0007	0.198	393	0.0007	0.202
	0.0005	0.198		0.0005	0.202
	0.0003	0.196		0.0003	0.197
601	0.0007	0.178	879	0.0007	0.173
	0.0005	0.180		0.0005	0.178
	0.0003	0.184		0.0003	0.178
1182	0.0007	0.178	1524	0.0007	0.148
	0.0005	0.178		0.0005	0.148
	0.0003	0.175		0.0003	0.151
1905	0.0007	0.156	2301	0.0007	0.148
	0.0005	0.156		0.0005	0.142
	0.0003	0.140		0.0003	0.131

Table 1: Identified parameter C from Hypothesis 1.

2.5 Functional dependence

After we verified that our model is consistent we analyze the functional dependence of k on μ. Our hypothesis assumes that the parameter C in (10) is constant. From Table 1 we see that C slightly varies. To analyze this variance we compute the arithmetic mean $E(C) = 0.171$ from values in Table 1. Then we compute the standard deviation $\sigma(C) = \sqrt{\left(1/8 \sum_i (C_i - E(C)^2\right)} = 0.021$ and the ratio $\sigma(C)/E(C)$ gives us the information in percents how C changes with respect to its mean value. In our case, $\sigma(C)/E(C) = 0.124$ which is 12%.

This variance could be caused by the irregularities in the mesh. However, C has decreasing tendency when increasing the mesh density and we clearly see very modest linear descent. Therefore we conclude that the parameter C is dependent on mesh density, however this dependence is weak.

REFERENCES

[1] P. Ahlrichs and B. Dunweg. Simulation of a single polymer chain in solution by combining lattice boltzmann and molecular dynamics. J. Chem. Phys., 17:8225–8239, 1999.

[2] A. Arnold, O. Lenz, S. Kesselheim, R. Weeber, F. Fahrenberger, D. Roehm, P. Koovan, and C. Holm. Espresso 3.1: Molecular dynamics software for coarse-grained models. In M. Griebel and M.A. Schweitzer, editors, Meshfree Methods for Partial Differential Equations VI, volume 89 of Lecture Notes in Computational Science and Engineering, pages 1–23. Springer Berlin Heidelberg, 2013.

[3] I. Cimrák, M. Gusenbauer, and T. Schrefl. Modelling and simulation of processes in microfluidic devices for biomedical applications. Computers and Mathematics with Applications, 64(3):278 – 288, 2012.

[4] M.M. Dupin, I. Halliday, C.M. Care, and L. Alboul. Modeling the flow of dense suspensions of deformable particles in three dimensions. Phys Rev E Stat Nonlin Soft Matter Phys., 75:066707, 2007.

[5] O. Etzmuss, J. Gross, and W. Strasser. Deriving a particle system from continuum mechanics for the animation of deformable objects. IEEE Transactions on Visualization and Computer Graphics, 9(4):538–550, October 2003.

[6] Z.G. Feng and E.E. Michaelides. The immersed boundary-lattice Boltzmann method for solving fluid-particles interaction problems. Journal of Computational Physics, 195:602–628, 2004.

[7] M. Gusenbauer, A. Kovacs, F. Reichel, L. Exl, S Bance, H. Ozelt, and T. Schrefl. Self-organizing magnetic beads for biomedical applications. Journal of Magnetism and Magnetic Materials, 324(6):977 – 982, 2012.

[8] S. Hénon, G. Lenormand, A. Richert, and F. Gallet. A new determination of the shear modulus of the human erythrocyte membrane using optical tweezers. Biophysics journal, 76(2):1145–1151, February 1999.

[9] L.D. Landau and E.M. Lifshitz. Electrodynamics of Continuous Media. Oxford-London-New York-Paris: Pergamon Press. X, 417 p., 1960. Translated from the Russian by J.B. Sykes and J.S. Bell.

[10] B.A. Lloyd, G. Székely, and M. Harders. Identification of spring parameters for deformable object simulation. Visualization and Computer Graphics, IEEE Transactions on, 13(5):1081–1094, September 2007.